The Journal of the Korean Institute of Electrical and Electronic Material Engineers Vol. 7, No. 1, pp.57-63,1994

# $Al_2O_3$ 絶緣薄膜의 形成과 그 活用方案에 관한 硏究

논 문
7-1-8

# A Study on the Growth of $Al_2O_3$ Insulation Films and Its Application

김 종 열*, 정 종 척*, 박 용 희*, 성 만 영*
(Jong-Ryeul Kim, Jong-Chuck Jung, Yong-Hee Park, Man-Young Sung)

**Abstract**

Aluminum oxide($Al_2O_3$) offers some unique advantages over the conventional silicon dioxide($SiO_2$) gate insulator: greater resistance to ionic motion, better radiation hardness, possibility of obtaining low threshold voltage MOS FETs, and possibility of use as the gate insulator in nonvolatile memory devices.

We have undertaken a study of the dielectric breakdown of $Al_2O_3$ on Si deposited by GAIVBE technique. In our experiments, we have varied the $Al_2O_3$ thickness from 300Å to 1400Å. The resistivity of $Al_2O_3$ films varies from $10^8$ ohm-cm for films less than 100Å to $10^{13}$ ohm-cm for flims on the order of 1000Å. The flat band shift is positive, indicating negative charging of oxide.

The magnitude of the flat band shift is less for negative bias than for positive bias. The relative dielectric constant was 8.5~10.5 and the electric breakdown fields were 6~7 MV/cm(+bias) and 11~12 MV/cm (-bias).

Key Words: $Al_2O_3$ Thin Film($Al_2O_3$ 박막,) Metal-$Al_2O_3$-Si(金屬-$Al_2O_3$), MAS Capacitor(MAS 커패시터)

## 1. INTRODUCTION

The use of silicon dioxide($SiO_2$) as an insulator has become so widespread in the microelectronics industry that it would seem almost unchangeable. Nevertheless, $SiO_2$ does not satisfy all criteria for an ideal technological insulator.

Therefore there have been investigations underway for some years by numerous workers searching for possible alternative insulators.[1-6]

Among those which have been seriously studied are phosphosilicate glass (PSG), silicon nitride ($Si_3N_4$), and aluminum oxide($Al_2O_3$).

We have $Al_2O_3$ films deposited by Gas Assisted and Ionized Vapor Beam Epitaxy (GAIVBE) technology at low temperature.[7-8] In this paper, details of the film deposition system and fundamental characteristics of the Al-$Al_2O_3$-Si structures were described and the dielectric breakdown of $Al_2O_3$ was studied.

## 2. SAMPLE PREPARATION

In our experiments, both n and p type silicon wafers of 4~6 ohm-cm resistivity were used. Films were deposited at different conditions (ionization currents, acceleration voltage, and substrate temperature) and films were also deposited on Si(100) for MOS structures. This technique is based on the formation of aluminum oxide when molten Al is evaporated in an oxygen atmosphere. Details of the GAIVBE system are described in Fig. 1.

Deposition chamber was evacuated by diffusion pump with cooled trap until $1.0\times10^{-7}$ torr. and Al evapolant(99.999%) was heated to 1200~1500℃ in the BN or Quartz crucible with nozzle of 0.5~

*: 고려대학교 전기공학과
접수일자: 1993年 8月 27日
심사완료: 1994年 1月 6日

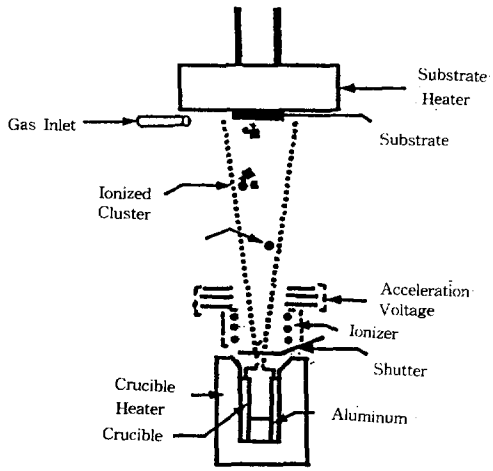


**Fig. 1** Schematic Diagram of the Gas Assisted and Ionized Vapor Beam Epitaxy System.

0.2mm in diameter and 1~3mm in length. Typical deposition conditions are listed in table 1.

Oxygen is then allowed into the vacuum chamber with the aid of a needle valve control near the substrate holder. When the vacuum pressure reach $1.5\times10^{-4}$ Torr., the needle valve control is set such that equilibrium is reached between the incoming oxygen and the outgoing gases. During the evaporation Al and oxygen molecules collide, increasing the aluminum oxide content of the evaporating gases. The efficiency of this collision process is determined by the capture cross sections of the particles involved and the partial pressure of the oxygen gas.

**Table 1.** Deposition Conditions for Gas Assisted and Ionized Vapor Beam Technique.

| | |
|---|---|
| Vacuum Pressure with $O_2$ Gas | $1\times10^{-4}$ Torr |
| Substrate Temperature | 150~650℃ |
| Acceleration Voltage | 0~5 kV |
| Ionizer Current | 0~1.5 A |
| Nozzle Size | 0.4~2.5 mm |
| Nozzle Length | (1-40)×Nozzle Size |
| Crucible Temperature | 1200~1500℃ |

It is therefore very important to allow the oxygen to flow through the system prior to evaporation so that the percentage of oxygen gas in the bell jar or near the substrate reaches a saturation value. The shutter is closed when the desired thickness of $Al_2O_3$ has been obtained on the substrate. After the oxide formation the substrate is placed in an oven at 150℃ for the post baking of a few min. This step is necessary to complete the oxide formation of Al molecules which did not interact with oxygen molecules during the evaporation.

In our experiments, the $Al_2O_3$ thicknesses were about 300~1400Å. The oxide thicknesses were determined ellipsometrically and varied by about 2% over the wafer for the 450Å oxides and as much as 5% over the wafer for the 900Å oxides. The samples had a heat treatment of 1000℃ for 30 minutes for annealing. As soon as possible, after the heat treatment, Al metallurgy is applied in the form of dots, in diameter, by evaporation followed by a post metallization annealing treatment of 400 ℃ for 30 minutes in $N_2$. All samples received a back contact of aluminum. The front contact was metallized with dot of aluminum. The samples used in our experiments had contact of thickness 1000Å with 0.080 cm diameter circular geometries, and area $2\times10^{-2}$ $cm^2$ (square geometries).

The index of refraction was determined to vary from 1.68 to 1.73 over the entire set of wafers by Abeles Measurement System.

The relative dielectric constant was calculated by measuring the diameter of the dot under the optical microscope. The relation

$$C=\frac{\varepsilon_r\varepsilon_0 A}{L}=\frac{\varepsilon_r\varepsilon_0}{L}\left(\frac{\pi}{4}d^2\right)$$

was then used to find the relative dielectric constant $\varepsilon_r$ where $\varepsilon_0$ = permittivity of vacuum = $8.85\times10^{-14}$ F/cm, L = oxide thickness, and d = diameter of metal dot on the $Al_2O_3$. The data taken over a number of capacitors on the same and on different wafers, gave a value of $\varepsilon_r$ ranging from 8.5 to 10.5. The resistivity of $Al_2O_3$ films varies from $10^8$ ohm-cm for films less than 100Å to $10^{13}$ ohm-cm for films on the order of 1000Å. Low temperature $Al_2O_3$ formation is performed by GAIVBE technique.

## 3. EXPERIMENTAL RESULTS AND DISCUSSIONS

The trapping of charge in the oxide is most readily observable in the time evolution C-V curves. The flat band shift $\triangle V_{FB}$ is a function of the trapped charge per unit area, Q, and its centroid relative to the metal interface. $\bar{x}$:

$$\triangle V_{FB} = - \frac{Q\bar{x}}{\varepsilon_0}$$

Note that a negative charge produces a positive flat band voltage shift, and a positive charge causes a negative flat band shift.

The initial C-V curve was recorded by sweeping the sample from accumulation to inversion and back to accumulation. Then the high field bias was applied for a given time. The C-V curve was recorded again by sweeping from accumulation to inversion and back.

Fig. 2 shows the results obtained by positive biasing a sample with an n-type substrate and Al electrodes. This graph demonstrates some typical features of the injection into $Al_2O_3$ layer. One can see from the curves that these are probably certain threshold biases below which almost no measurable flatband shift occurs for a given time.

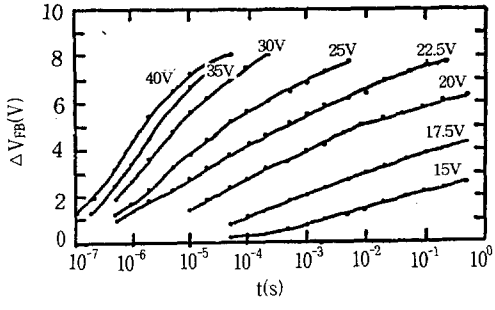


**Fig. 2** Flatband shift with log t for Al-(500 Å)$Al_2O_3$-n-Si with positive applied voltages as parameter.

Above this threshold bias, we observe a flat band shift as a function of the injection time. For applied voltages above the threshold bias, the flat band shift $\triangle V_{FB}$ can, over a limited range, be written as approximately proportional to logarithm of the injection time, t. Over the range of applied voltage from 15V to 22.5V, the slopes of the curves are approximately the same. For $V_G$>22.5V the slopes of the curves increase with applied voltages. These curves suggest that there are three injection regions : a subthreshold region, an above threshold region in which $\triangle V_{FB} \propto$ log t and a high field region which has a different injection mechanism.

Fig. 3 shows the results obtained with negative bias on a sample with a p-type substrate and Al electrodes. This has the same general features shown in Fig. 2.

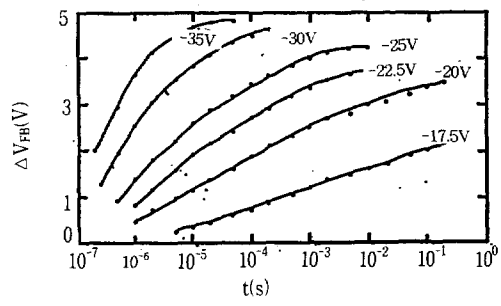


**Fig. 3** Flatband shift with log t for Al-(500 Å)$Al_2O_3$-p-Si with negative applied voltages as parameter.

Note that in both Fig. 2 and Fig. 3 the flat band shift is positive, indicating negative charging of the oxide. Note also that the magnitude of the flat band shift is less for negative bias(Fig. 3) than for positive bias(Fig. 2).

One method of studying dielectric breakdown is to apply a constant high voltage to the sample and observe the I-t behavior. Fig. 4 shows the behavior of the current for an applied bias of +22V on 500Å film of $Al_2O_3$ with Al metallization and n-Si substrate.

After the application of bias the current first rises rapidly to a peak(which is much greater than that shown in Fig. 4 because of the X-Y recorder's relatively slow response time) and then decays monotonically. At t=80s, we see a sharp rise in the current, corresponding to electrical breakdown of the $Al_2O_3$.

This is a typical result obtained with Al electrodes. In some samples, we observed a small fluctuation in current prior to breakdown, similar to what Tsujide et al.[9] reported. We were not able to see this fluctuation in all cases. Fig. 5 shows a

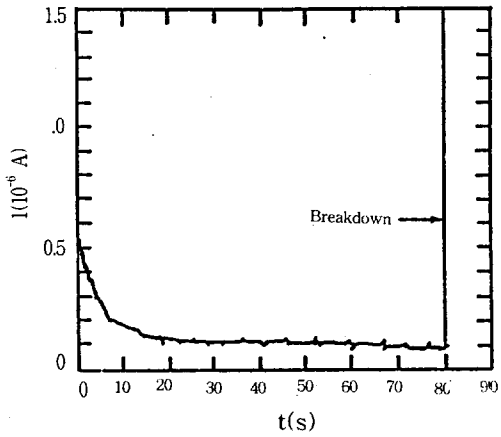


**Fig. 4** Current(I) vs. time(t) for +22V bias on Al-(500Å) $Al_2O_3$-n-Si.

typical I-t curve obtained with a gold electrode. The spikes in the curve correspond to self-quenching breakdowns(SQBD)[10]. Note that the SQBD's tend to occur with greater frequency as t increases.

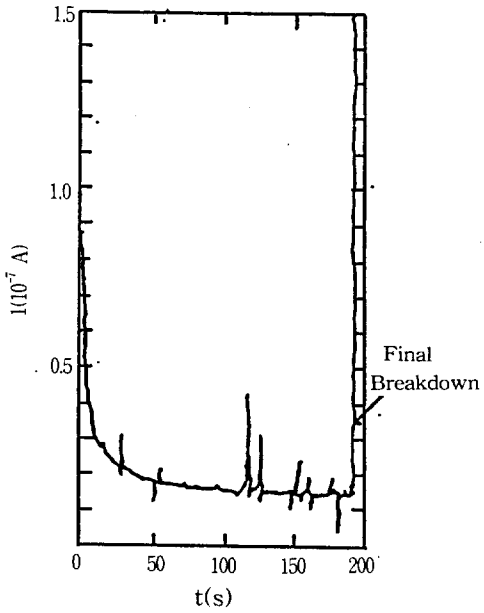


**Fig. 5** Typical current decay for +27.5V bias on Au-(500Å)$Al_2O_3$-n-Si.

Although we have found it easy to produce SQBD's in samples with Au electrodes, we have never observed them in samples with Al electrodes. The final breakdown is not necessarily a shorting breakdown in all cases, but might be described as the switching from a low-conductivity to a high-conductivity state. This can be seen in Fig. 6, which shows C-V curves taken before and after the breakdown event, for negative bias applied to a p-Si substrate, with Al electrode.

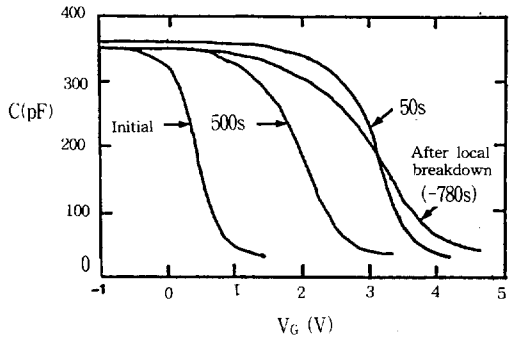


**Fig. 6** Typical pre- and post- breakdown C-V curves for -20V bias on Al-(500Å) $Al_2O_3$-p-Si.

Note the initial increase in $\triangle V_{FB}$ up to 25-50s, followed by a decrease, shown by the curves moving to the left. This is a typical result obtained with negative bias.

Note that there is a stretchout of the C-V curve as well as a shift after breakdown. We have observed both positive and negative shifts with negative bias.

Fig. 7 shows the C-V curves before and after breakdown for positive bias on p-Si samples. Incandescent illumination was used to maintain an inversion layer.

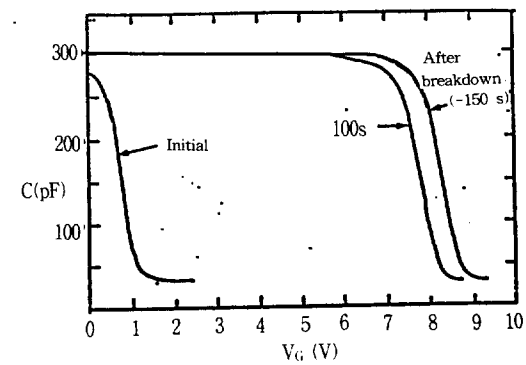


**Fig. 7** Typical pre- and post- breakdown C-V curves for +18V bias on Al-(500Å) $Al_2O_3$-p-Si.

Fig. 8 shows the pre- and post- breakdown curves for an n-Si sample positively biased with Al electrode. The hump of the post- breakdwon curve is due to capacitance meter being "fooled" by the large leakage current. Fig. 8 and Fig. 9 show the typical results for negative bias applied to a Au-plated oxide. Here again we observe a negative flat band shift immediately following breakdown. In this case there is also distortion of the C-V curve.

The determination of the breakdown strength of $Al_2O_3$ is not straightforward. The usual method of applying a voltage ramp to the MOS capacitor and measuring the voltage at which the sample breaks down is not adequate. Because of charging effects, the breakdown voltage measured by the ramp technique will depend on the ramp rate; the greater the ramp rate, the greater will be the breakdown voltage. An alternative method is to apply a fixed bias and measure the time to breakdown. By making a series of such measurements at different biases, we obtain curves such as are displayed in Fig. 10.

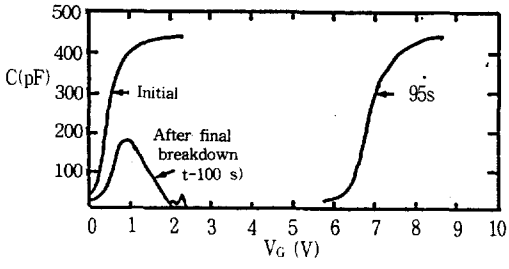


**Fig. 8** Typical pre- and post- breakdown C-V curves for +22V bias on Al-(500Å) $Al_2O_3$-n-Si.

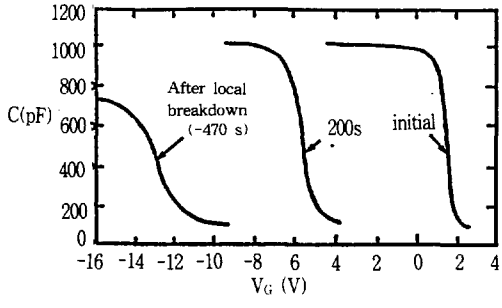


**Fig. 9** Typical pre- and post- breakdown C-V curves for -32.5V bias on Au-(500Å) $Al_2O_3$-p-Si.

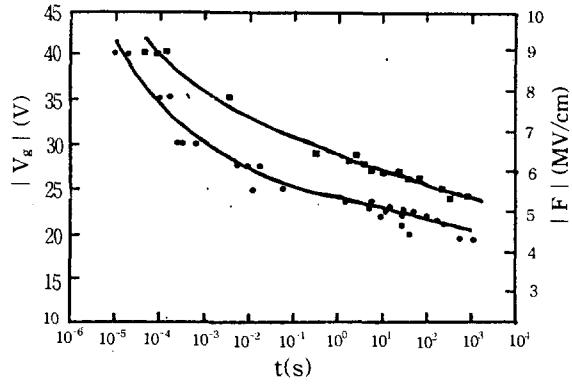


**Fig. 10** Applied field, E vs. time to breakdown, t.
●:positive bias Al-(500Å) $Al_2O_3$-n-Si.
■:negative bias Al-(500Å) $Al_2O_3$-p-Si.

As the curves do not approach a limiting field as $t \rightarrow \infty$, we shall define the breakdown field at an arbitrary time, such as $t = 10^3$s. The quoted breakdown field is the average field in the oxide, not the maximum field. Note also that there is a difference of 1MV/cm in the breakdown field between for negative bias and for positive bias. Observation of Fig. 10 shows that the breakdown field is about 4.5MV/cm for positive bias and about 5 MV/cm for negative bias on Si.

Measurements made with Au electrodes give approximately the same value of breakdown field as with Al electrode for positive bias on n-Si, but a value of 6.5MV/cm for negative bias on p-Si.

## 4. CONCLUSIONS

Aluminum oxide ($Al_2O_3$) offers some unique advantages over the conventional silicon dioxide ($SiO_2$) gate insulation; possibility of obtaining low threshold-voltage MOSFETs, and possibility of use as the gate insulator in nonvolatile memory devices. We have undertaken a study of the high field properties of $Al_2O_3$ on Si deposited by GAI-VBE technique.

Our test structures were metal-aluminumoxide-silicon capacitors with both aluminum and gold field plates. The major problem with $Al_2O_3$, when used as a gate insulator, is its flat band voltage instability under moderate bias levels (>1MV/cm).

This is caused by trapping of electrons in the

oxide.

We have explored the mechanism of charge injection and trapping from both a theoretical and an experimental viewpoint.

We biased metal-$Al_2O_3$-Si samples to various conditions of electric field and determined the time evolution of flat band voltage and its dependence on the field.

The results indicated threshold field for charge injection of about 1.5MV/cm for positive bias with Al electrodes. From the polarity of the flat band shifts we know that the trapped charge is negative in sign and the charges are undoubtedly electrons. The data also indicate that it is electron injection from the cathode which dominates low field conduction.

In this paper, the dielectric breakdown of $Al_2O_3$ was also studied. It was found that, because of the continuous buildup of space charge, a consistent determination of breakdown strength could not be made using a ramp voltage waveform. Instead, a study was done of the time to breakdown for given fixed bias. The average fields required to produce breakdown in $10^3$ sec were approximately 4.5MV/cm for positive bias on either Al or Au field plates, 5.0 MV/cm for negative bias on Al, and 6.5 MV/cm for negative bias on Au.

※ 본 연구는 한국전력공사의 연구비 지원에 의해 수행되었음.

## REFERENCES

1) N.M. Johnson and M.A. Lampert; J.Appl. Phys., 46, 1216 (1975)
2) S.M. Sze; Physics of Semiconductor Devices, John Wiley and Sons Inc.(1985)
3) E.H. Nicollian and C.N. Berglund; J. Appl. Phys., 41, 3052 (1970)
4) D.J. Maria, J.M. Aitken and D.R. Young; J. Appl. Phys., 47, 2740 (1976)
5) W.S. Johnson and J.H. Gibbons; Projected Range Statistics and Related Materials, 2nd Edition, John Wiley and Sons. Inc.(1975)
6) R.H. Walden; J. Appl. Phys., 43, 3(1972)
7) M.Y. Sung et al; 15th Int. Conf. on Metallurgical Coatings and 1988 Vacuum Metallurgy Conf. on Special Meeting, April 11-15, 1988 San Diego CA.
8) M.Y. Sung et. al; 35th National Symposium American Vacuum Society Oct, 3-7, 1988, Atlanta, GA.
9) T. Tsujide, S. Nakanuma and Y. Ikushima; J. Electrochem. Soc., 117(5), 703(1970)
10) H. Kampshoff etc.; "Conduction and Charging Behavior in MA(O)S System" , J. Electrochem. Soc., 24, 1761(1977)
11) M.Y. Sung and B. Cowell; J. Vacuum Science and Tech., A-7,(3), 792(1989).
12) S. Singh and K.V. Anand; Thin Sol. Films, 37, 453(1976).
13) A.K. Sinha, W.S. Lindenberger, W.D. Powell, and E.I. Povilonis; J. Electrochem.Soc., 2046 (1980).
14) J. Kolk and E.L. Heasel; Solid St. Elect., Vol.23, pp.101-107 (1980).
15) Walter C. Johnson; Princeton Univ. New Jersey, pp.33,(1978).
16) E. Harari and B.S.H. Royce; Solid St. and Materials Lab. Princ. Univ., pp.280(1980).